

Probing anisotropic superfluidity of rashbons in atomic Fermi gases

Hui Hu¹, Lei Jiang², Xia-Ji Liu¹, and Han Pu²

¹ARC Centre of Excellence for Quantum-Atom Optics,
Centre for Atom Optics and Ultrafast Spectroscopy,

Swinburne University of Technology, Melbourne 3122, Australia

²Department of Physics and Astronomy, and Rice Quantum Institute, Rice University, Houston, TX 77251, USA

(Dated: October 22, 2018)

Motivated by the prospect of realizing a Fermi gas of ⁴⁰K atoms with a synthetic non-Abelian gauge field, we investigate theoretically a strongly interacting Fermi gas in the presence of a Rashba spin-orbit coupling. As the two-fold spin degeneracy is lifted by spin-orbit interaction, bound pairs with mixed singlet and triplet pairings (referred to as rashbons) emerge, leading to an anisotropic superfluid. We show that this anisotropic superfluidity can be probed via measuring the momentum distribution and single-particle spectral function in a trapped atomic ⁴⁰K cloud near a Feshbach resonance.

PACS numbers: 05.30.Fk, 03.75.Hh, 03.75.Ss, 67.85.-d

Owing to the unprecedented experimental controllability, ultracold atoms have been proven to be an ideal table-top system to study some long-sought, challenging many-body problems. A well-known example is the non-perturbative problem of crossover from a Bose-Einstein condensation (BEC) to a Bardeen-Cooper-Schrieffer (BCS) superfluidity in an ultracold atomic Fermi gases [1]. Here we study a strongly interacting Fermi gas in the presence of a synthetic non-Abelian gauge field, as motivated by the recent demonstration of such field in bosonic ⁸⁷Rb atoms [2] and the prospect of its realization in fermionic ⁴⁰K atoms [3]. We focus on the Rashba spin-orbit (SO) interaction and explore its impact on the unitary Fermi gas.

A weak non-Abelian gauge field such as Rashba SO interaction is well understood. It was shown in 2001 by Gor'kov and Rashba [4] that a condensed matter system of superconducting 2D metals with weak SO coupling features a mixed spin singlet-triplet pairing field, and its spin magnetic susceptibility can be dramatically affected by the SO interaction. By applying an additional large Zeeman magnetic field, it was proposed by Zhang *et al.* [5] and Sato *et al.* [6] that a topological phase with gapless edge states and non-Abelian Majorana fermionic quasiparticles may form. More recently, Vyasankere and Shenoy identified an interesting bound state by solving the two-body problem [7], referred to as *rashbons*. By increasing the strength of SO coupling, a BCS superfluid can therefore evolve into a BEC of rashbons [8].

In this Letter, we investigate the salient features of rashbons by using a functional path-integral functional method. We identify clearly rashbons from the gaussian fluctuations of pairing field and show they possess anisotropic effective mass. We demonstrate at the saddle-point level that the condensation of rashbons gives rise to both singlet and triplet pairings. As a result, the momentum distribution and single-particle spectral function become highly anisotropic. By performing calculations for a realistic system of trapped ⁴⁰K fermions at a Feshbach

resonance, we present observable experimental signatures for visualizing the anisotropic superfluidity of rashbons.

The model — Let us start by formulating the BEC-BCS crossover with a Rashba SO coupling $\mathcal{H}_{so} = \lambda(\hat{k}_y\hat{\sigma}_x - \hat{k}_x\hat{\sigma}_y)$, whose Hamiltonian is given by,

$$\mathcal{H} = \int d\mathbf{r} \left\{ \psi^\dagger [\xi_{\mathbf{k}} + \mathcal{H}_{so}] \psi + U_0 \psi_\uparrow^\dagger \psi_\downarrow^\dagger \psi_\downarrow \psi_\uparrow \right\}, \quad (1)$$

where $\xi_{\mathbf{k}} = \hbar^2 \hat{k}^2 / (2m) - \mu$, and $\psi(\mathbf{r}) = [\psi_\uparrow(\mathbf{r}), \psi_\downarrow(\mathbf{r})]$ denotes collectively the fermionic field operators. The contact *s*-wave interaction ($U_0 < 0$) occurs between un-like spins. We use the functional path integral method [9] and consider the action $\mathcal{Z} = \int \mathcal{D}[\psi, \bar{\psi}] \exp \{-S[\psi(\mathbf{r}, \tau), \bar{\psi}(\mathbf{r}, \tau)]\}$, where $S[\psi, \bar{\psi}] = \int_0^\beta d\tau \int d\mathbf{r} \sum_\sigma \bar{\psi}_\sigma(\mathbf{r}) \partial_\tau \psi_\sigma(\mathbf{r}) + \mathcal{H}(\psi, \bar{\psi})$, $\beta = 1/(k_B T)$, and $\mathcal{H}(\psi, \bar{\psi})$ is obtained by replacing the field operators ψ^\dagger and ψ with the Grassmann variables $\bar{\psi}$ and ψ , respectively. The interaction term can be decoupled by using the standard Hubbard-Stratonovich transformation with the introduction of a fluctuating pairing field $\Delta(\mathbf{r}, \tau)$. It is convenient to use the 4-dimensional Nambu spinor $\Phi(\mathbf{r}, \tau) \equiv [\psi_\uparrow, \psi_\downarrow, \bar{\psi}_\uparrow, \bar{\psi}_\downarrow]$ and rewrite the action as, $\mathcal{Z} = \int \mathcal{D}[\Phi, \bar{\Phi}; \Delta, \bar{\Delta}] \exp \{-\int_0^\beta d\tau \int d\mathbf{r} \left[\frac{1}{2} \bar{\Phi} (-\mathcal{G}^{-1}) \Phi - \frac{|\Delta|^2}{U_0} \right] - \beta \sum_{\mathbf{k}} \xi_{\mathbf{k}}\}$, where \mathcal{G} is the single-particle Green function.

By integrating out the fermionic field, the effective action is $\mathcal{Z} = \int \mathcal{D}[\Delta, \bar{\Delta}] \exp \{-S_{eff}[\Delta, \bar{\Delta}]\}$, where $S_{eff} = \int_0^\beta d\tau \int d\mathbf{r} \left\{ -\frac{|\Delta(\mathbf{r}, \tau)|^2}{U_0} \right\} - \frac{1}{2} \text{Tr} \ln [-\mathcal{G}^{-1}] + \beta \sum_{\mathbf{k}} \xi_{\mathbf{k}}$. To proceed, we restrict ourselves to the gaussian fluctuation and expand $\Delta(\mathbf{r}, \tau) = \Delta_0 + \delta\Delta(\mathbf{r}, \tau)$. The effective action is then approximated by $S_{eff} = S_0 + \Delta S$, where the saddle-point action $S_0 = \int_0^\beta d\tau \int d\mathbf{r} \left(-\frac{\Delta_0^2}{U_0} \right) - \frac{1}{2} \text{Tr} \ln [-\mathcal{G}_0^{-1}] + \beta \sum_{\mathbf{k}} \xi_{\mathbf{k}}$ and, in the momentum space, the fluctuation action takes the form $[k \equiv (\mathbf{k}, i\omega_m)$ and $q \equiv (\mathbf{q}, i\nu_n)$]: $\Delta S = \sum_{\mathbf{q}, i\nu_n} \left[-\frac{1}{U_0} \delta\Delta(q) \delta\bar{\Delta}(q) \right] +$

$\frac{1}{2} \left(\frac{1}{2}\right) \text{Tr}_\sigma \sum_{k,q} [\mathcal{G}_0(k) \Sigma(q) \mathcal{G}_0(k-q) \Sigma(-q)]$, where

$$\Sigma(q) = \begin{bmatrix} 0 & i\delta\Delta(q) \hat{\sigma}_y \\ -i\delta\bar{\Delta}(-q) \hat{\sigma}_y & 0 \end{bmatrix}. \quad (2)$$

Rashbon — Let us consider first the normal state with $\Delta_0 = 0$, in which case the Green function reduces to its non-interacting form as $\mathcal{G}_0(k) = \text{Diag}\{\hat{g}_0(k), -\hat{g}_0(-k)\}$ with $\hat{g}_0(k) = [i\omega_m - \xi_{\mathbf{k}} - \lambda(k_y \hat{\sigma}_x - k_x \hat{\sigma}_y)]^{-1}$, leading to *two* helicity branches in the single-particle spectrum, $E_{\mathbf{k},\alpha} = \xi_{\mathbf{k}} + \alpha\lambda k_\perp$, where $k_\perp \equiv (k_x^2 + k_y^2)^{1/2}$ and $\alpha = \pm 1$. The fluctuation action is given by $\Delta S = \sum_q [-\Gamma^{-1}(q)] \delta\Delta(q) \delta\bar{\Delta}(q)$, where $\Gamma^{-1}(q)$ is the inverse vertex function which, at $\mathbf{q} = \mathbf{0}$, takes the form

$$\Gamma^{-1}(\omega) = \frac{m}{4\pi\hbar^2 a_s} - \frac{1}{V} \sum_{\mathbf{k}} \left[\sum_{\alpha=\pm} \frac{1/2 - f(E_{\mathbf{k},\alpha})}{\omega^+ - 2E_{\mathbf{k},\alpha}} + \frac{1}{2\epsilon_{\mathbf{k}}} \right],$$

where $f(x) = 1/(e^{x/k_B T} + 1)$ is the Fermi distribution function and we have renormalized the bare interaction U_0 by the *s*-wave scattering length, $1/U_0 = m/(4\pi\hbar^2 a_s) - V^{-1} \sum_{\mathbf{k}} 1/(2\epsilon_{\mathbf{k}})$, with V being the quantization volume.

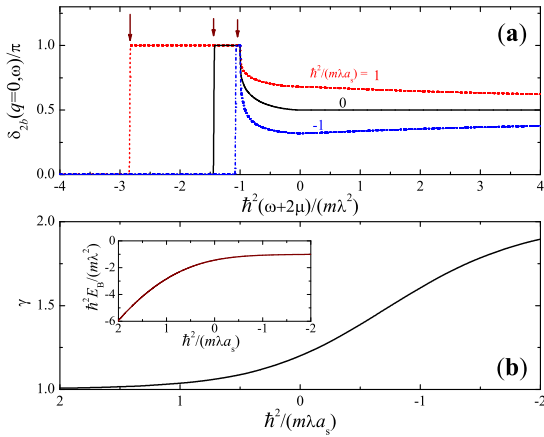


Figure 1: (Color online) (a) Rashbons as evidenced by the two-body phase shift of $\Gamma^{-1}(\mathbf{0}, \omega)$ at three different scattering lengths. The arrows indicate the position of binding energy. (b) Effective mass of rashbons [$\gamma = M_\perp/(2m)$] in the strong SO limit. The inset shows the bound state energy as a function of the scattering length.

The vertex function is simply the Green function of the fermion pair. A bound state can therefore be examined clearly by calculating the phase shift [10] $\delta(\mathbf{q}, \omega) = -\text{Im} \ln[-\Gamma^{-1}(\mathbf{q}, i\nu_n \rightarrow \omega + i0^+)]$. For a true boson, the phase shift is given by $\delta_B(\mathbf{q}, \omega) = \pi\Theta(\omega - \epsilon_{\mathbf{q}}^B + \mu_B)$, where $\epsilon_{\mathbf{q}}^B$ and μ_B are the bosonic dispersion and chemical potential, respectively, and $\Theta(x)$ is the step function. In Fig. 1(a), we plot the two-body part of the phase shift at $\mathbf{q} = \mathbf{0}$, obtained by discarding Fermi functions. The phase shift jumps from 0 to π at a critical frequency, resembling that of a true boson. This is exactly the demonstration of a bound state, or rashbon. By recalling that

the bosonic chemical potential is given by $\mu_B = 2\mu - E_B$, where E_B is the bound state energy, the critical frequency $(\omega + 2\mu)_c$ at $\mathbf{q} = \mathbf{0}$ gives exactly E_B . Using the fact that the critical frequency corresponds to the position where $\text{Re}[\Gamma^{-1}]$ changes sign, we have

$$\frac{m}{4\pi\hbar^2 a_s} - \frac{1}{2V} \sum_{\mathbf{k}; \alpha=\pm} \left[\frac{1}{E_B - 2E_{\mathbf{k},\alpha}} + \frac{1}{\epsilon_{\mathbf{k}}} \right] = 0. \quad (3)$$

The inset in Fig. 1(b) shows the bound state energy as a function of the SO coupling strength. At the unitarity limit, the bound state energy is universally given by $E_B(a_s = \pm\infty) \approx -1.439229m\lambda^2/\hbar^2$. The size of rashbons a is therefore at the order of $\hbar^2/(m\lambda)$. Rashbons are well defined once $a \ll k_F^{-1}$ or $\lambda k_F \gg \epsilon_F$. Thus, we anticipate that the system will cross over to a gas of rashbons at $\lambda k_F/\epsilon_F \sim 1$.

In the limit of a large SO coupling, the well-defined rashbons should have a bosonic dispersion $\epsilon_{\mathbf{q}}^B = \hbar^2 q_\perp^2/(2M_\perp) + \hbar^2 q_z^2/(2M_z)$ and weakly interact with each other *repulsively*. Because of the anisotropic fermionic dispersion $E_{\mathbf{k},\pm} = \xi_{\mathbf{k}} \pm \lambda k_\perp$, the effective mass of rashbons becomes anisotropic. While $M_z = 2m$ is not affected by the Rashba coupling, M_\perp may get strongly renormalized. As the jump of the phase shift at nonzero \mathbf{q} which occurs at $(\omega + 2\mu)_c - \epsilon_{\mathbf{q}}^B$, we can numerically determine M_\perp . Fig. 1(b) reports $\gamma = M_\perp/(2m)$. At unitarity, we find $\gamma \simeq 1.2$. When the system becomes an ensemble of weakly interacting rashbons, the heavy mass M_\perp causes a decrease in the condensation temperature so that $T_{\text{BEC}} = \gamma^{-2/3} T_{\text{BEC},0}$, where $T_{\text{BEC},0} \simeq 0.218 T_F$ is the BEC temperature without the SO coupling.

Condensation of rashbons — Let us now turn to the condensed phase characterized by a nonzero order parameter $\Delta_0 \neq 0$. At the mean-field saddle-point level, the single-particle Green function takes the form,

$$\mathcal{G}_0^{-1} = \begin{bmatrix} i\omega_m - \xi_{\mathbf{k}} - \mathcal{H}_{so} & i\Delta_0 \hat{\sigma}_y \\ -i\Delta_0 \hat{\sigma}_y & i\omega_m + \xi_{\mathbf{k}} - \mathcal{H}_{so}^* \end{bmatrix}. \quad (4)$$

The inversion of the above matrix can be worked out explicitly, leading to *two* single-particle Bogoliubov dispersions whose degeneracy is lifted by the SO interaction, $E_{\mathbf{k},\pm} = \sqrt{(\xi_{\mathbf{k}} \pm \lambda k_\perp)^2 + \Delta_0^2}$, and the normal and anomalous Green functions from which we can immediately obtain the momentum distribution $n(\mathbf{k}) = 1 - \sum_{\alpha} [1/2 - f(E_{\mathbf{k},\alpha})] \gamma_{\mathbf{k},\alpha}$ and the single-particle spectral function $A_\uparrow(\mathbf{k}, \omega) = A_\downarrow(\mathbf{k}, \omega) = \sum_{\alpha} [(1 + \gamma_{\mathbf{k},\alpha}) \delta(\omega - E_{\mathbf{k},\alpha}) + (1 - \gamma_{\mathbf{k},\alpha}) \delta(\omega + E_{\mathbf{k},\alpha})] / 4$, where $\gamma_{\mathbf{k},\pm} = (\xi_{\mathbf{k}} \pm \lambda k_\perp) / E_{\mathbf{k},\pm}$. The chemical potential and the order parameter are to be determined by the number and the gap equations, $n = \sum_{\mathbf{k}} n(\mathbf{k})$ and $\Delta_0 = -U_0 \Delta_0 \sum_{\alpha} [1/2 - f(E_{\mathbf{k},\alpha})] / (2E_{\mathbf{k},\alpha})$, respectively. Fig. 2 displays the chemical potential and order parameter as functions of the SO coupling strength for a unitary Fermi gas. The increase of the SO strength

leads to a deeper bound state. In analogy with the BEC-BCS crossover, the order parameter and critical transition temperature are greatly enhanced once the rashbons are well defined at $\lambda k_F \sim \epsilon_F$. In the large SO coupling limit, the chemical potential can be written as $\mu = E_B/2 + \mu_B/2$, where the chemical potential of rashbons μ_B is positive due to the repulsion between rashbons and decreases with increasing coupling as shown in the inset of Fig. 2(c). By assuming an *s*-wave repulsion with scattering length a_B , where $\mu_B \simeq (n/2)4\pi\hbar^2 a_B/M$, we estimate within mean-field that in the unitarity limit, $a_B \simeq 3\hbar^2/(m\lambda)$, comparable to the size of rashbons. A more accurate description of the interaction between two rashbons can be obtained by solving a four-fermion problem.

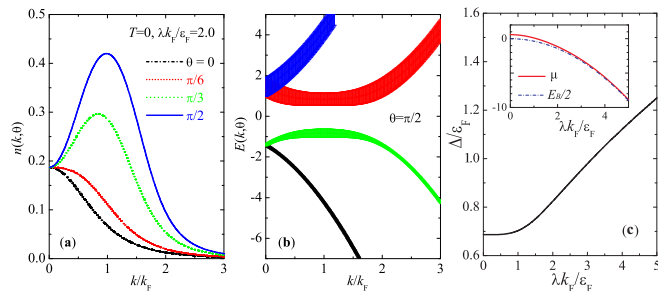


Figure 2: (a) Momentum distribution and (b) single-particle spectral function for $\theta = \pi/2$ at $\lambda k_F/\epsilon_F = 2$. Here θ is the angle between \mathbf{k} and the z -axis. The width of the curves in (c) represents the weight factor $(1 \pm \gamma_{\mathbf{k},\pm})/4$ for each of the four Bogoliubov excitations. (c) Mean-field order parameter as a function of the SO coupling for a homogeneous unitary Fermi gas at zero temperature. The inset shows the chemical potential and the half of bound state energy, in units of ϵ_F .

Figure 2(a) and (b) illustrate the momentum distribution and the single-particle spectral function, respectively. These quantities exhibit anisotropic distribution in momentum space due to the SO coupling and can be readily measured in experiment.

Another important consequence of the SO coupling is that the pairing field contains both a singlet and a triplet component [4, 8]. For the system under study, it is straightforward to show that the triplet and singlet pairing fields are given by $\langle \psi_{\mathbf{k}\uparrow} \psi_{-\mathbf{k}\uparrow} \rangle = -i\Delta_0 e^{-i\varphi_{\mathbf{k}}} \sum_{\alpha} \alpha [1/2 - f(E_{\mathbf{k},\alpha})]/(2E_{\mathbf{k},\alpha})$ and $\langle \psi_{\mathbf{k}\uparrow} \psi_{-\mathbf{k}\downarrow} \rangle = \Delta_0 \sum_{\alpha} \alpha [1/2 - f(E_{\mathbf{k},\alpha})]/(2E_{\mathbf{k},\alpha})$, respectively, where $e^{-i\varphi_{\mathbf{k}}} \equiv (k_x - ik_y)/k_{\perp}$. The magnitude of these are shown in Fig. 3. The weight of the triplet component increases as the SO coupling strength increases and becomes equal to that of the singlet component in the strong SO coupling limit.

Probing the anisotropic superfluidity of rashbons — One leading candidate to observe superfluid rashbons is a trapped Fermi gas of ^{40}K atoms near a broad Feshbach resonance, where an applicable scheme to generate the Rashba SO coupling was recently proposed [3]. Pre-

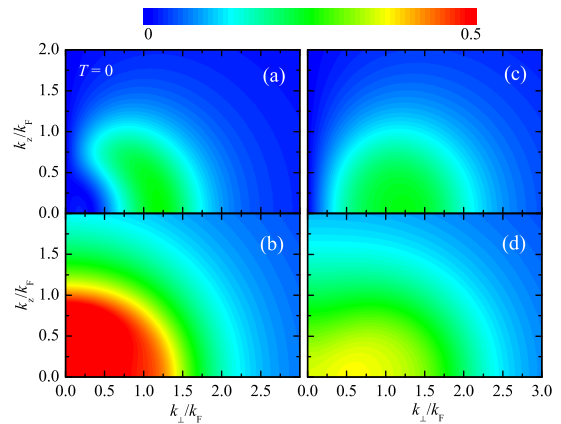


Figure 3: (Color online) Linear contour plot for the triple pairing correlation $|\langle \psi_{\mathbf{k}\uparrow} \psi_{-\mathbf{k}\uparrow} \rangle|$ between like spins (upper panel) and the singlet pairing correlation $|\langle \psi_{\mathbf{k}\uparrow} \psi_{-\mathbf{k}\downarrow} \rangle|$ between unlike spins (lower panel) for a homogeneous unitary Fermi gas at zero temperature. The SO coupling strength in (a) and (b) is $\lambda k_F/\epsilon_F = 1$, and in (c) and (d) is $\lambda k_F/\epsilon_F = 2$.

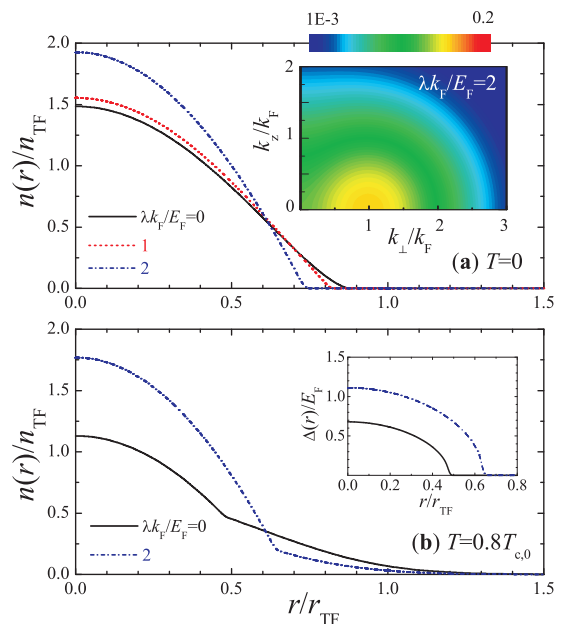


Figure 4: (Color online) Density distributions of a trapped unitary Fermi gas at zero $T = 0$ (a) and finite temperature $T = 0.8T_{c,0}$ (b) and at different SO coupling strengths. $T_{c,0}$ is the critical temperature in the absence of the SO coupling. The inset in (a) shows log-scale contour plot of the momentum distribution and the inset in (b) illustrates the profile of the order parameter at finite temperature. Here the Fermi energy is given by $E_F = (3N)^{1/3}\hbar\omega_0$, Fermi wave number $k_F = (24N)^{1/6}a_{ho}^{-1}$, Thomas-Fermi radius $r_{TF} = (24N)^{1/6}a_{ho}$, and the non-interacting peak density $n_{TF} = (24N)^{1/2}/(3\pi^2)a_{ho}^{-3}$, where $a_{ho} = \sqrt{\hbar/(m\omega)}$ is the characteristic length of the harmonic oscillator.

vious experiments have demonstrated the measurement of momentum distribution and single-particle spectral function is ^{40}K in the absence of the SO coupling [11]. We perform the mean-field calculation in a 3D spherical harmonic trap $V_T(r) = m\omega_0^2 r^2/2$, by using the local density approximation (LDA). In LDA, the gas was divided into small cells with a local chemical potential $\mu(r) = \mu - V_T(r)$. The local density $n(r)$, momentum distribution $n(\mathbf{k}; r)/(2\pi)^3$, occupied spectral function $A(\mathbf{k}, \omega; r)f(\omega)k^2/(2\pi^2)$ are then integrated over the whole space to obtain the total contribution. The chemical potential at the trap center μ can be determined by the number equation $\int dr n(r) = N$, where N is the total number of fermions. We show, in Fig. 4, the density profile of a trapped unitary Fermi gas at different SO coupling strengths and temperatures. As anticipated, with the increase of the SO coupling the cloud shrinks. The anisotropic momentum distribution at large SO coupling, which can be measured using the time-of-flight technique, can still be clearly seen as illustrated in the inset of Fig. 4(a).

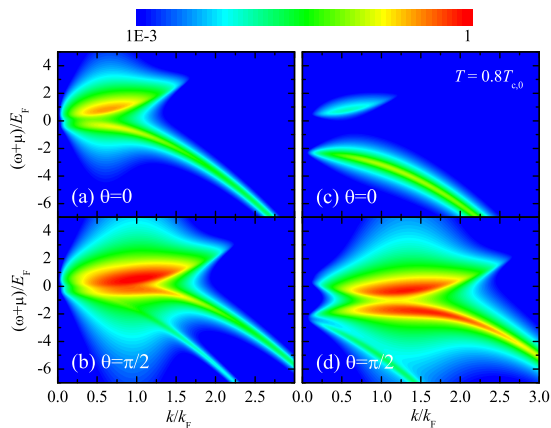


Figure 5: (Color online) Log-scale contour plot of the single-particle spectral function for a trapped unitary Fermi gas at $T = 0.8T_{c,0}$. The SO coupling strength in (a) and (b) is $\lambda k_F/E_F = 1$, and in (c) and (d) is $\lambda k_F/E_F = 2$.

Figure 5 presents the occupied spectral function at $T = 0.8T_{c,0}$, where $T_{c,0}$ is the critical temperature without the SO interaction. The distinct behavior for the spectral function at $\theta = 0$ (along the z -axis) and $\pi/2$ (in the transverse plane) can be probed by the recently demonstrated momentum-resolved rf-spectroscopy [11]. To make better comparison with the experiment, we have included in the calculation an energy resolution of $0.2E_F$, as presented in the JILA rf-measurement. Our calculations therefore clearly demonstrate that the anisotropic nature of the rashbon superfluid will not be smeared out by averaging over the trapped cloud.

Summary — We have shown that rashbons induced by a strong Rashba spin-orbit coupling differ significantly from the BEC-BCS crossover molecules studied over the

past few years. Rashbons have anisotropic effective mass and condense into a mixed singlet-triplet pairing state. They lead to a strong anisotropy in the momentum distribution and the single-particle spectral function. We have proposed that these distinct behaviors can be readily probed in a strongly interacting Fermi gas of ^{40}K atoms in a synthetic non-Abelian gauge field.

More interesting features of rashbons may be discovered thanks to the unprecedented controllability in ultracold atoms. Rashbons in 2D may be utilized to create Majorana fermions [5, 12]. Rashbons under a magnetic field may exhibit inhomogeneous superfluidity with mixed singlet-triplet pairings and their properties may be greatly affected by the field. Therefore, the exploration of strong correlation effects of rashbons is a new exciting many-body problem. In the current work, we have adopted a mean-field approach. The mean-field calculation in the condensed phase can be improved by incorporating gaussian pair fluctuations [13].

Acknowledgment — HH and XJL was supported by the ARC Discovery Projects No. DP0984522 and No. DP0984637. HP is supported by the NSF and the Welch Foundation (Grant No. C-1669). We would like to thank Chuanwei Zhang, Hui Zhai and Shizhong Zhang for useful discussions.

Note added: After we completed our work, we became aware of the work reported in Ref. [14] which treats a similar system. Our results agree with each other where they overlap.

-
- [1] S. Giorgini, L. P. Pitaevskii, and S. Stringari, Rev. Mod. Phys. **80**, 1215 (2008).
 - [2] Y.-J. Lin *et al.*, Phys. Rev. Lett. **102**, 130401 (2009); Y.-J. Lin, K. Jimenez-Garcia, and I. B. Spielman, Nature (London) **471**, 83 (2011).
 - [3] J. D. Sau *et al.*, Phys. Rev. B **83**, 140510(R) (2011).
 - [4] L. P. Gor'kov, and E. I. Rashba, Phys. Rev. Lett. **87**, 037004 (2001).
 - [5] C. Zhang *et al.*, Phys. Rev. Lett. **101**, 160401 (2008).
 - [6] M. Sato, Y. Takahashi, and S. Fujimoto, Phys. Rev. Lett. **103**, 020401 (2009); Phys. Rev. B **82**, 134521 (2010).
 - [7] J. P. Vyasankere, and V. B. Shenoy, Phys. Rev. B **83**, 094515 (2011).
 - [8] J. P. Vyasankere, S. Zhang and V. B. Shenoy, arXiv:1104.5633 (2011).
 - [9] C. A. R. Sá de Melo, Mohit Randeria, and Jan R. Engelbrecht, Phys. Rev. Lett. **71**, 3202 (1993).
 - [10] P. Nozières and S. Schmitt-Rink, J. Low Temp. Phys. **59**, 195 (1985).
 - [11] J.T. Stewart, J.P. Gaebler, and D.S. Jin, Nature **454**, 744 (2008); J.P. Gaebler *et al.*, Nature Phys. **6**, 569 (2010).
 - [12] S. Tewari *et al.*, arXiv:1012.0057 (2010); M. Gong, S. Tewari, and C. Zhang, arXiv:1105.1796 (2011).
 - [13] H. Hu, X.-J. Liu, and P. D. Drummond, Europhys. Lett. **74**, 574 (2006).
 - [14] Z.-Q. Yu, and H. Zhai, arXiv:1105.2250 (2011).